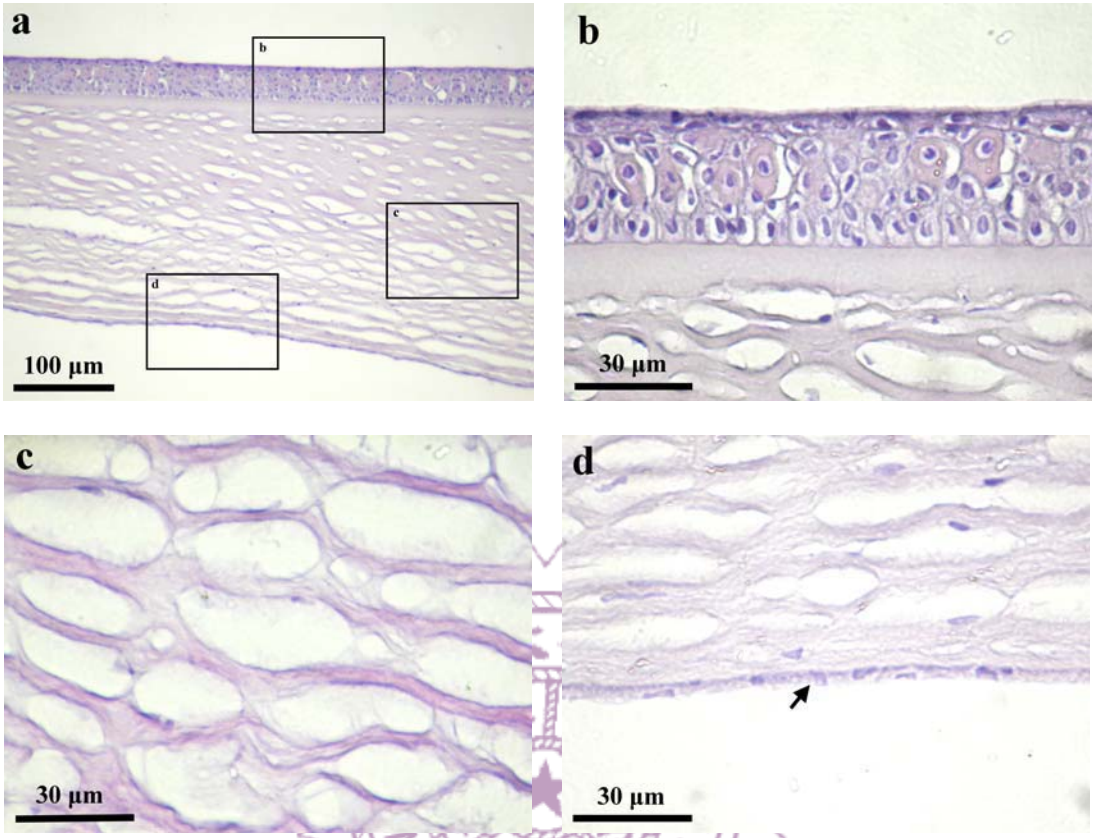

Fig 1. The paraffin sections of the adipose eyelids with H&E staining. (a) The adipose eyelid is composed of three layers: the outer and inner layers are epithelial tissue and the middle layer is the connective tissue; (b) The outer layer is composed of multiple stacks of epithelial cells; (c) The connective tissue of the middle layer; (d) the single stack of epithelial tissue of the inner layer (as indicated by the arrow).

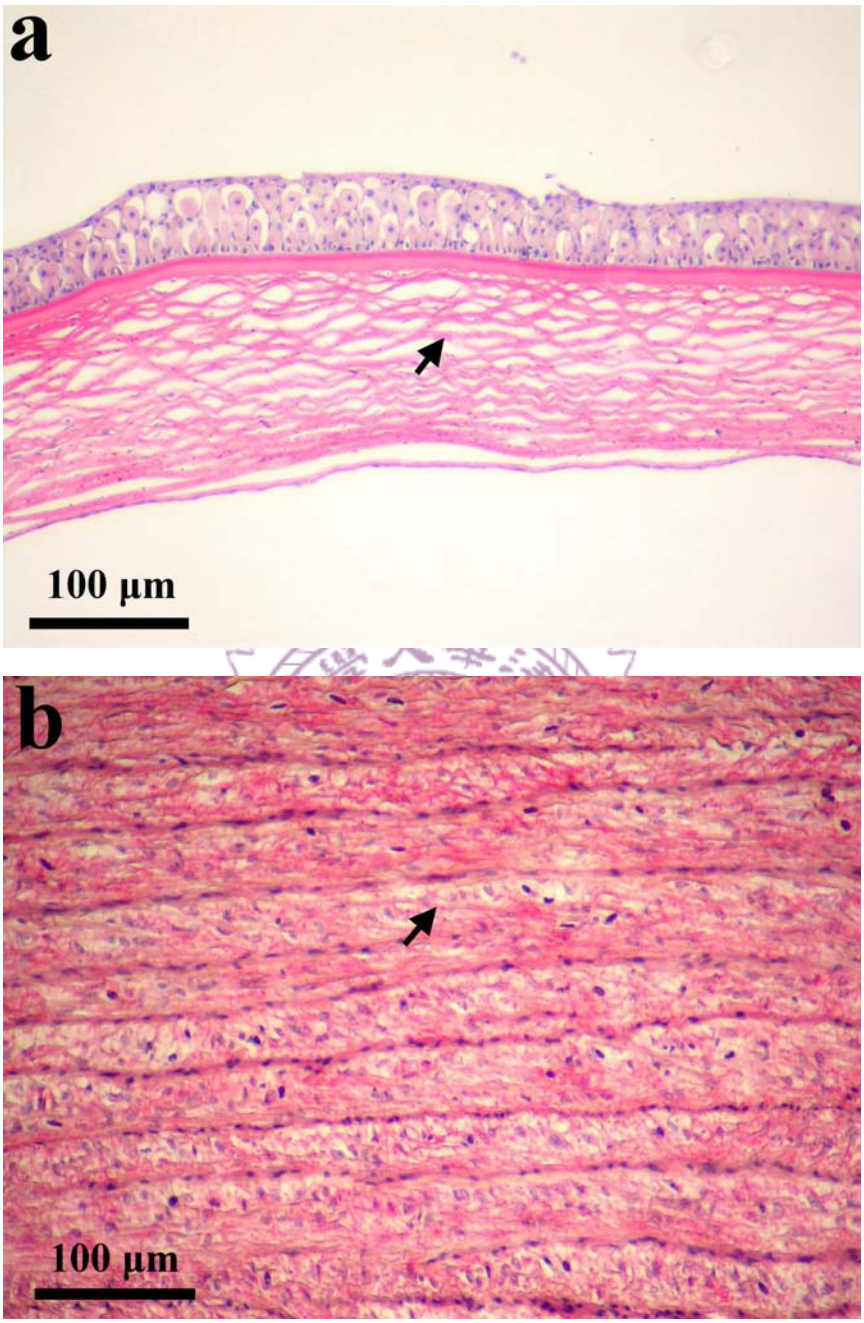

Fig 2. The paraffin section of (a) the milkfish adipose eyelid and (b) the artery of the chicken stained with Pico-Ponceau with Hematoxylin staining. The red part (as indicated by the arrow) indicates the collagen fibers or connective fibers of the connective tissue.

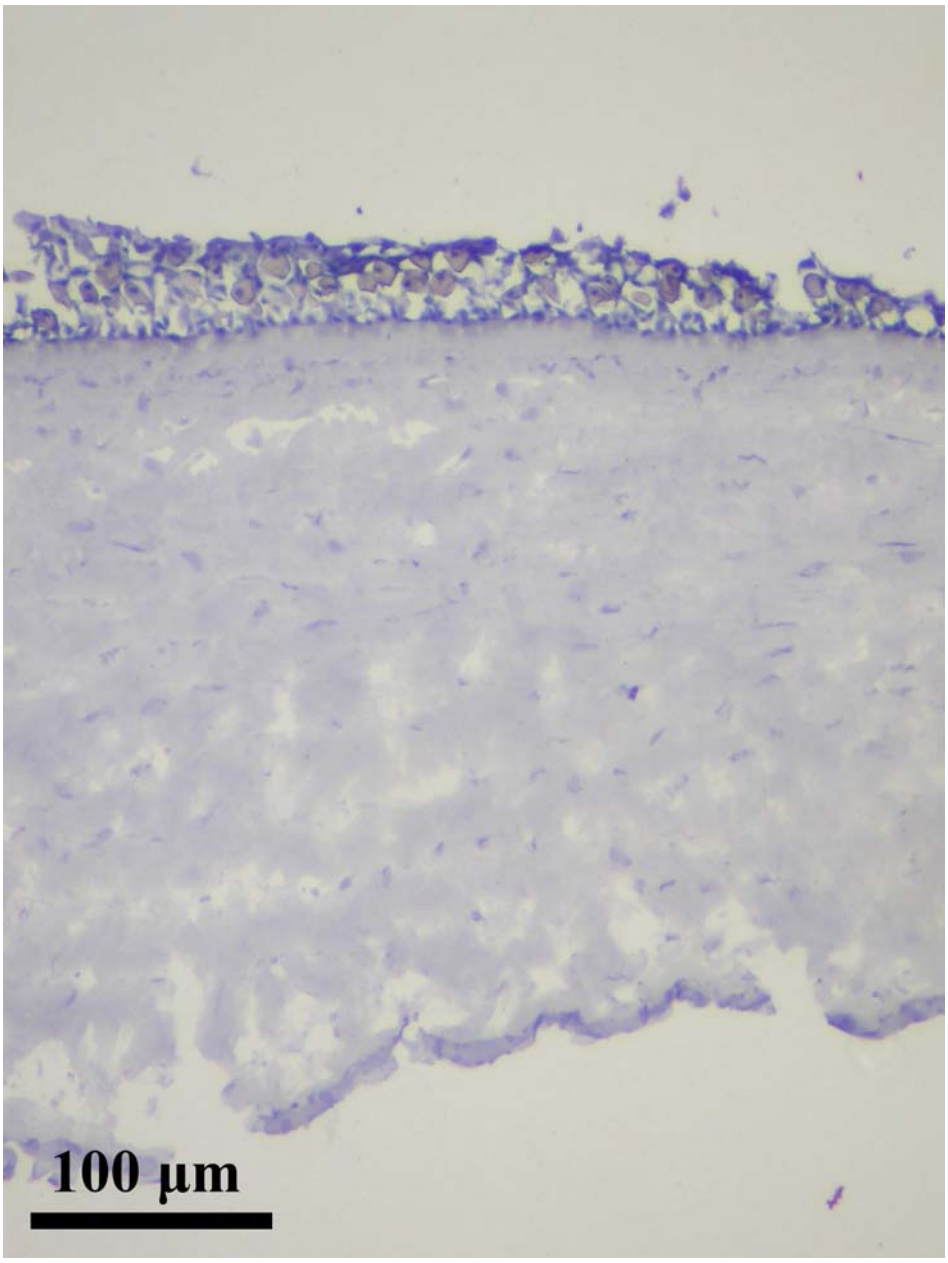

Fig 3. The cryo-section of adipose eyelid with Oil Red O staining. The absent of the red color part indicates the adipose eyelid doesn't contain the adipose tissue.

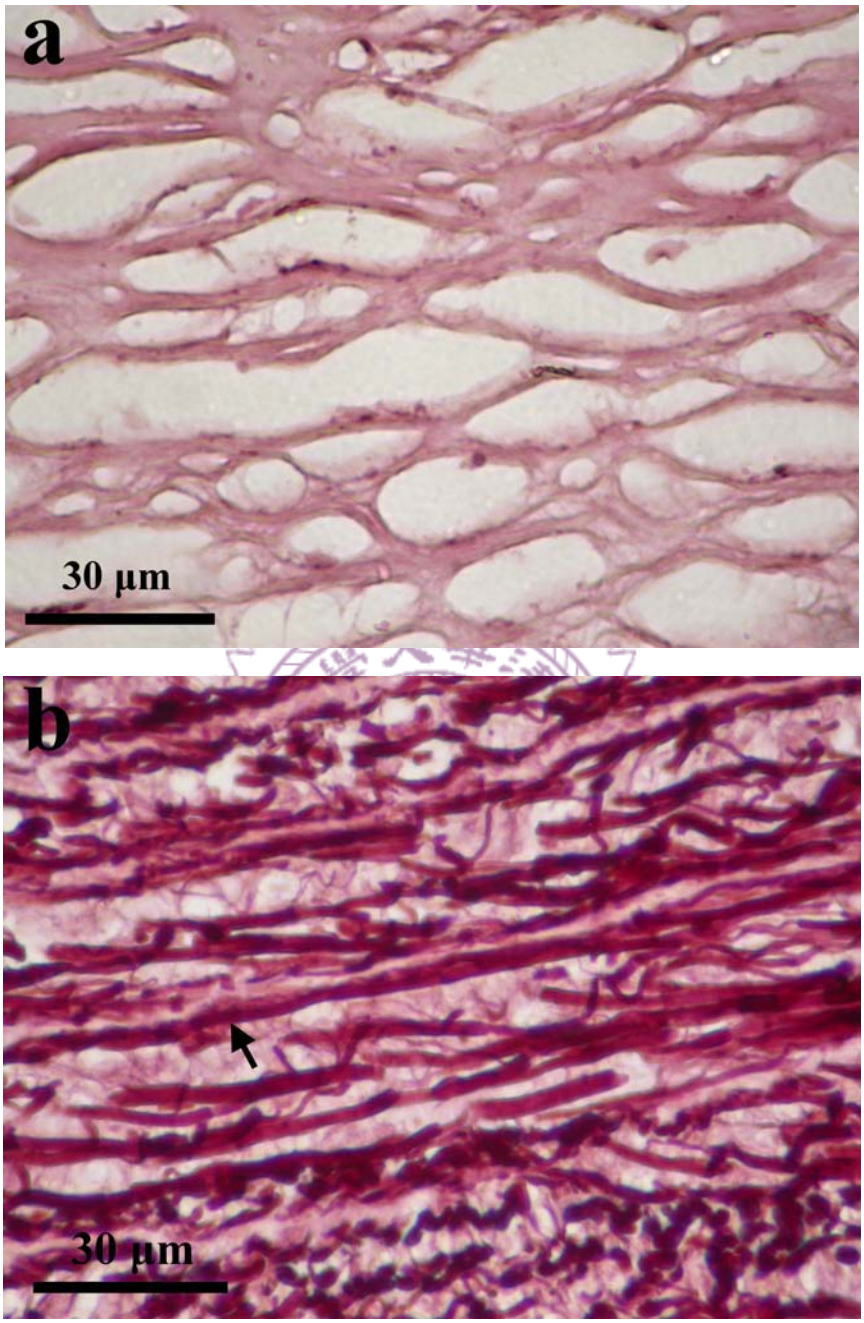

Fig 4. The paraffin section of the milkfish adipose eyelid (a) and the artery (b) with Orcein staining. The dark purple lines highlight the presence of elastic fiber (as indicated by the arrow) in (b) which is absent in the adipose eyelid section but present in the artery section.

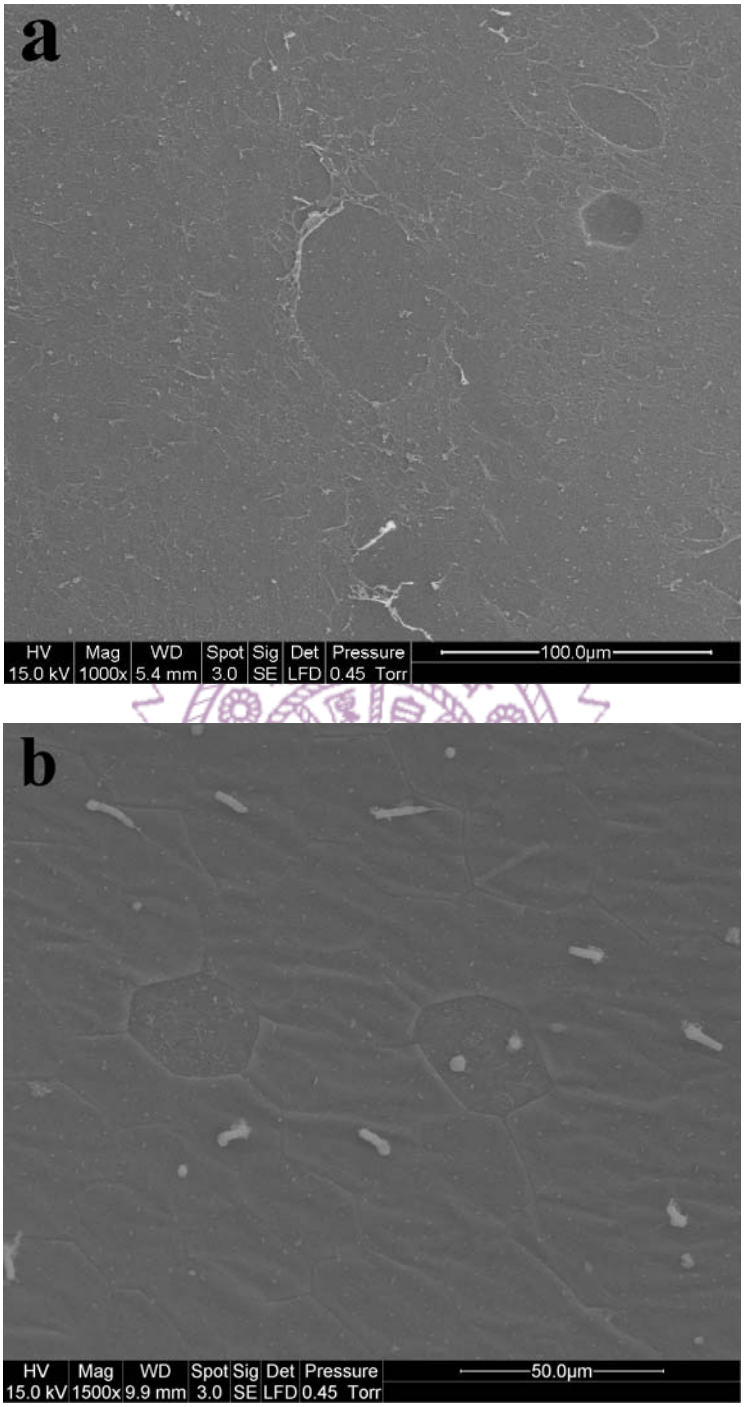

Fig 5. The SEM photos of the adipose eyelid as viewed from (a) the outer and (b) inner side. The typical epithelial cells only could be observed from the inner side.

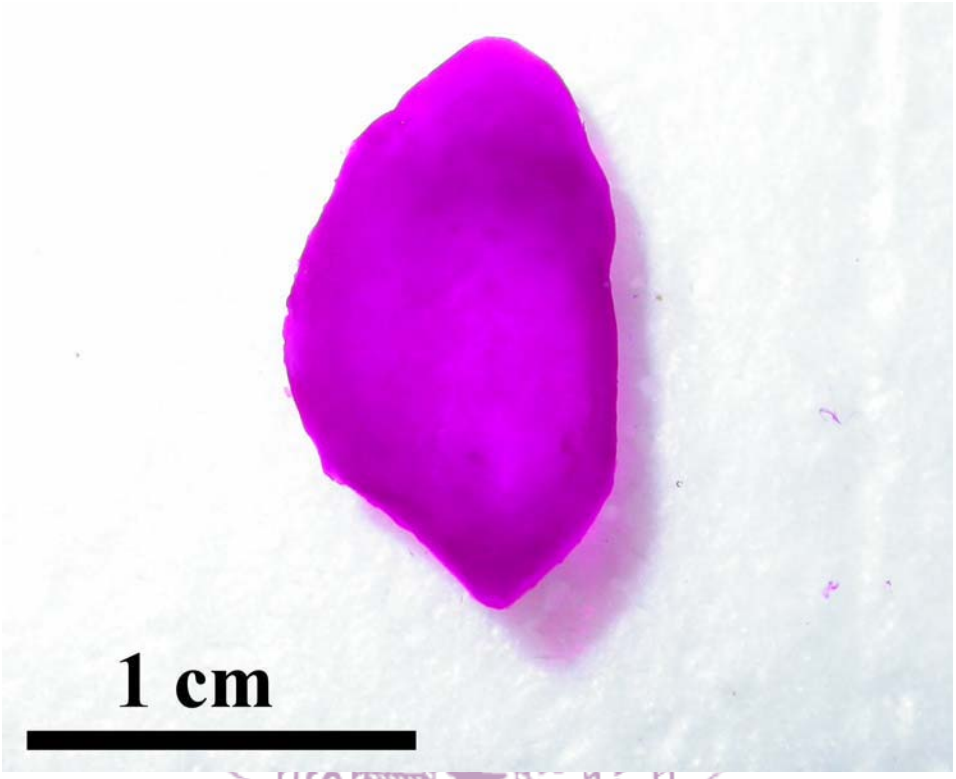

Fig 6. The adipose eyelid with PAS staining which is the stain for the carbohydrates.

The red color indicates the carbohydrates are present in the adipose eyelid.

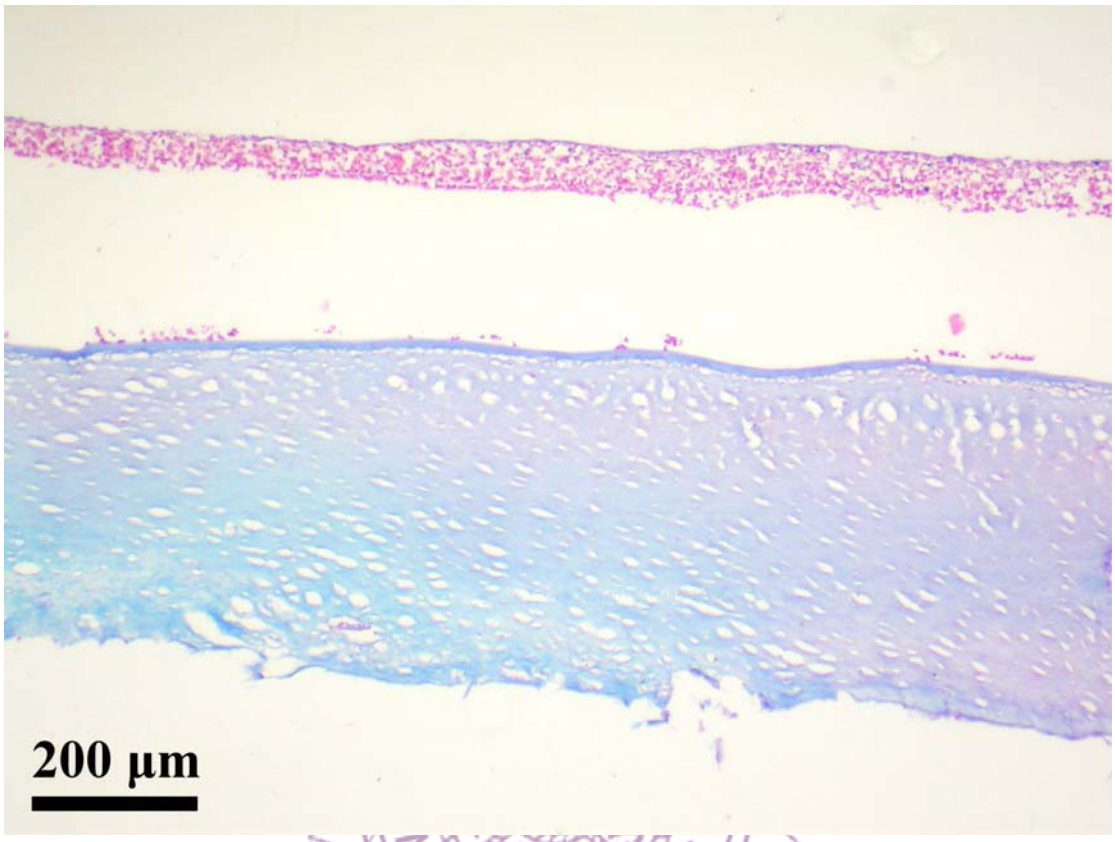

Fig 7. The paraffin section of adipose eyelid with Alcian Blue pH 2.8 staining which is the stain for the acid mucosubstances. The red part shows the nuclei of the outer multiple epithelial tissues, and the blue part indicates the acid mucosubstances are present in the adipose eyelid.

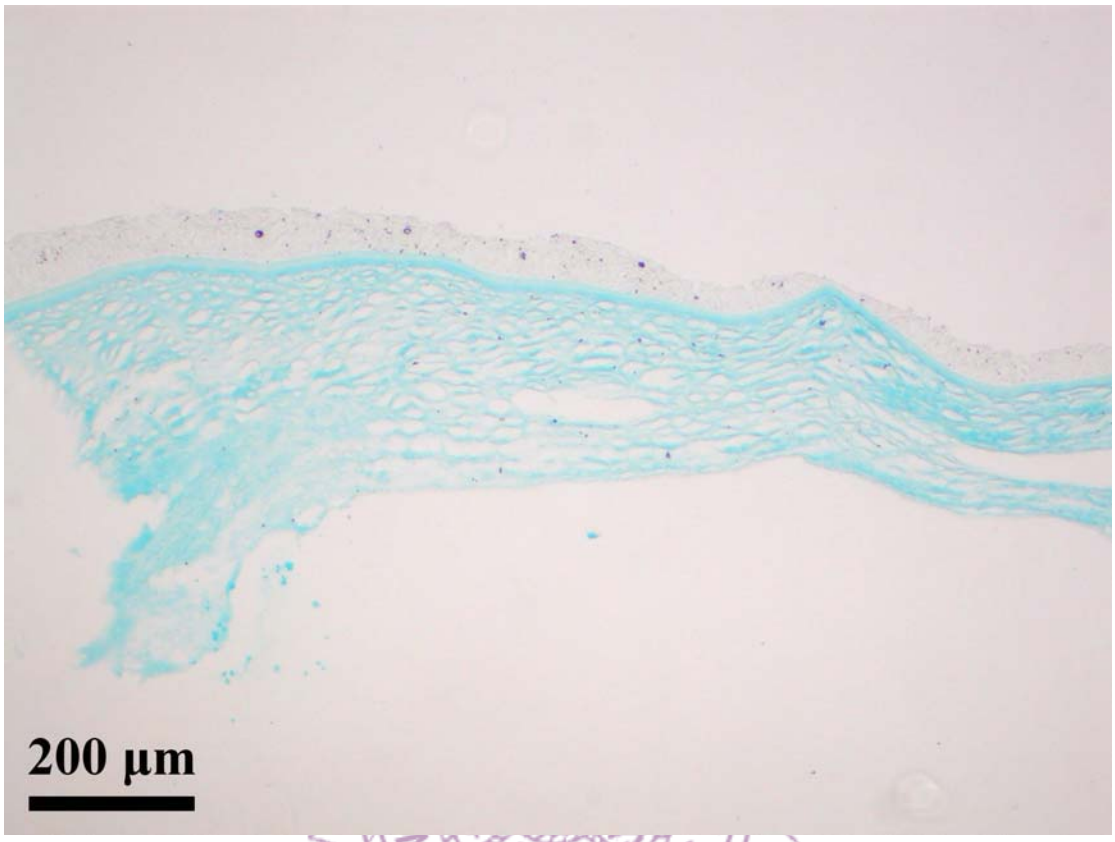

Fig 8. The paraffin section of adipose eyelid with Alcian Blue pH 1.0 staining which is the stain for the sulfated mucosubstances. The blue part indicates the sulfated mucosubstances are present in the adipose eyelid.

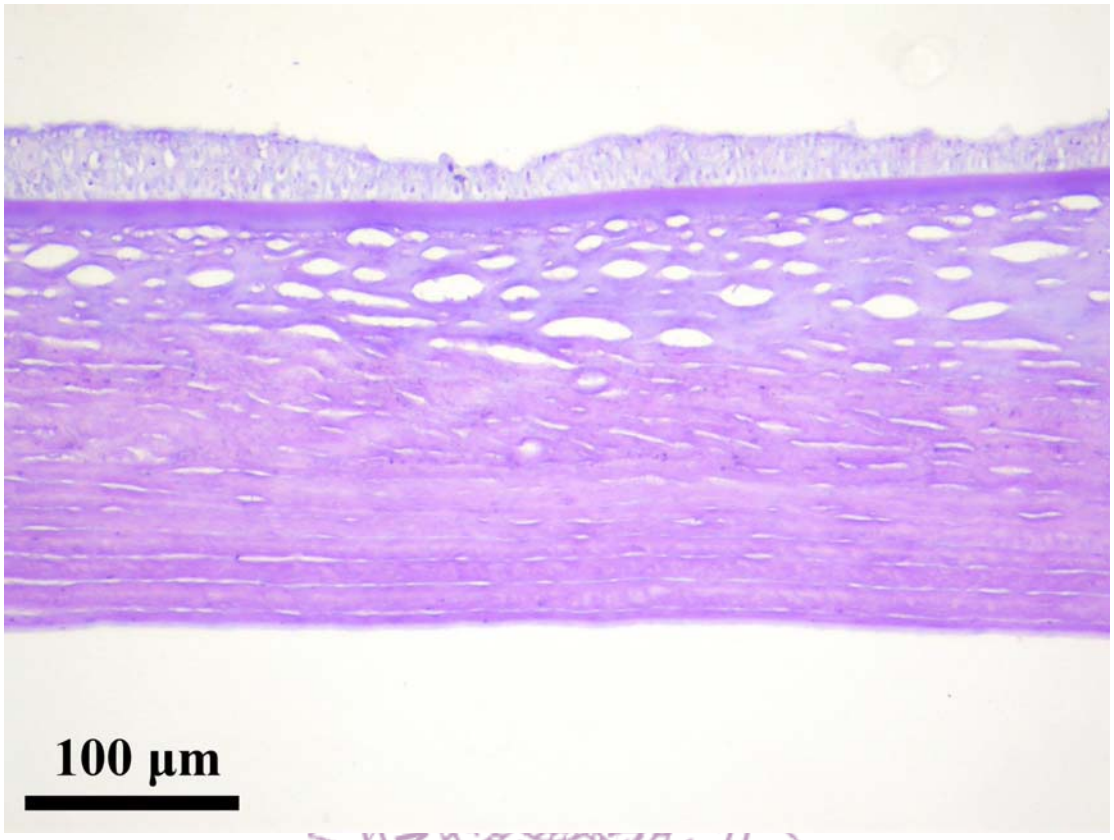

Fig 9. The adipose eyelid with Aldyhyde Fuchsin-Alcian Blue staining which is the stain for identifying different levels of sulfated mucosubstances. The purple part indicates the weakly sulfated mucosubstances are present in the adipose eyelid.

Fig 10. The lyophilized collagen extracted from the milkfish adipose eyelids.

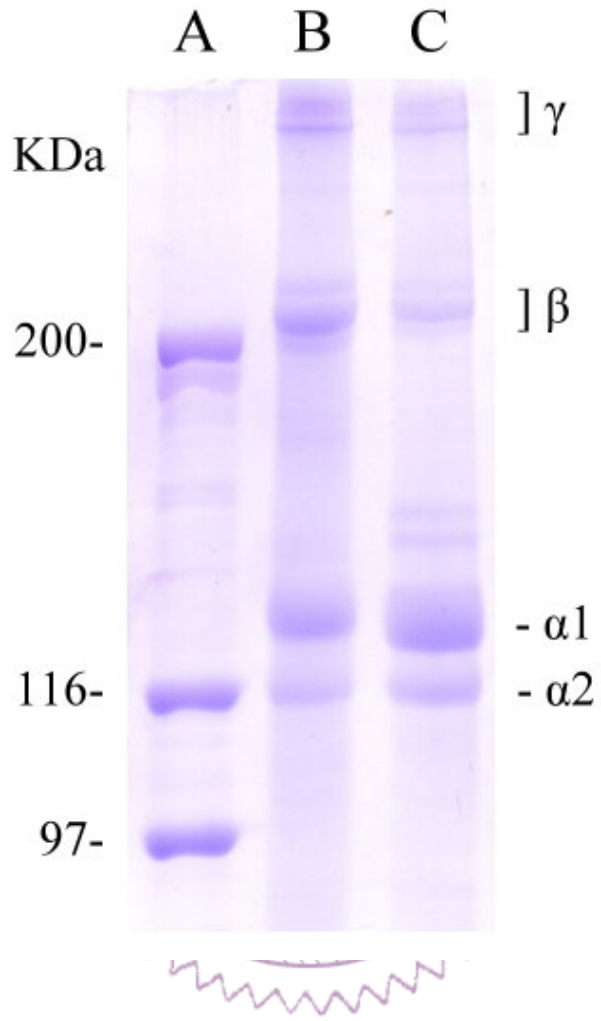

Fig 11. SDS-PAGE electrophoresis gels of the calf skin type I collagen and the milkfish adipose eyelid collagen. (A) protein marker, (B) calf skin type I collagen, (C) milkfish adipose eyelid collagen.

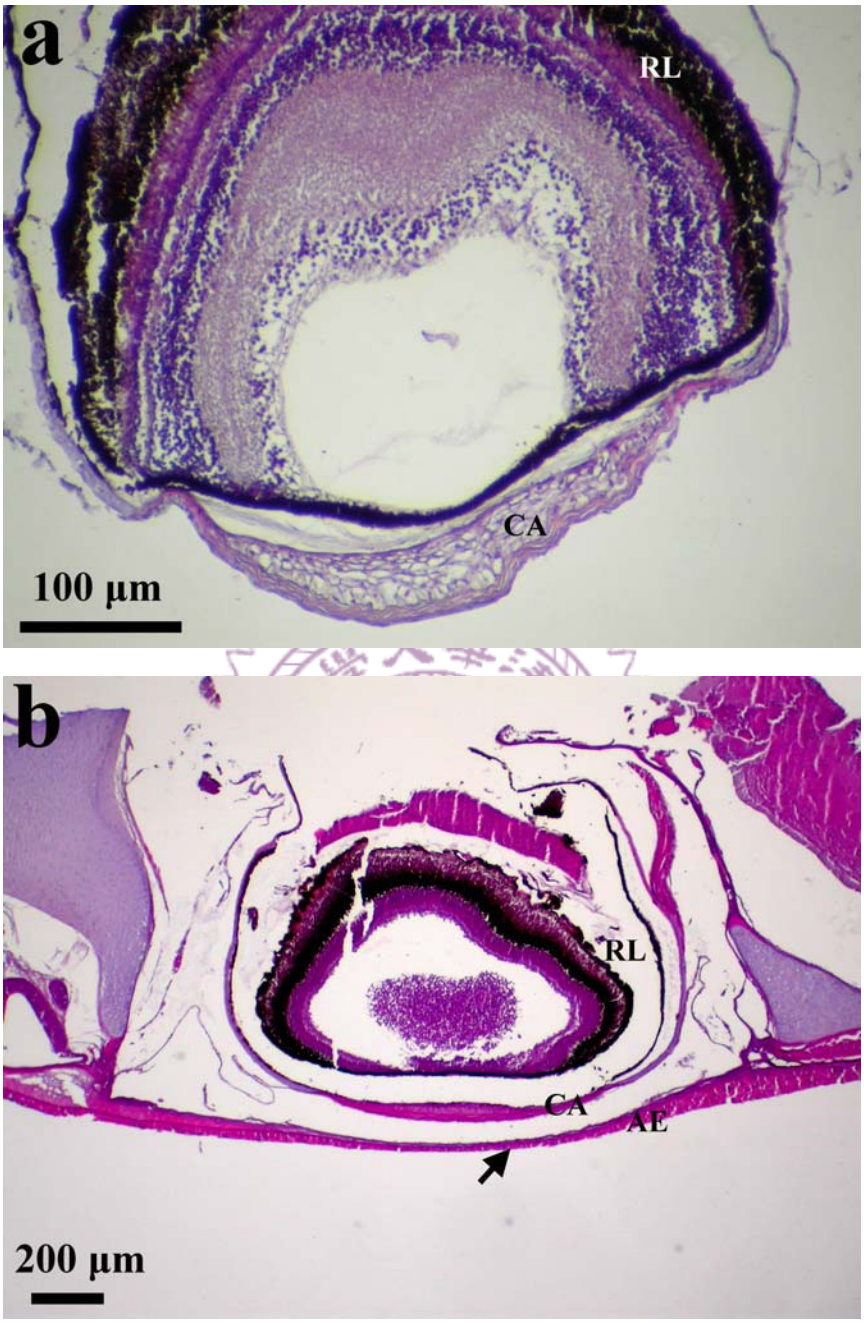

Fig 12. The sagittal section of the larval milkfish head (a) and the juvenile milkfish head (b) with H&E staining. Arrow in (b) indicates the presence of the adipose eyelid(AE). (AE: adipose eyelid; CA: cornea; RL: retinal layer. See Fig 15 for details of RL).

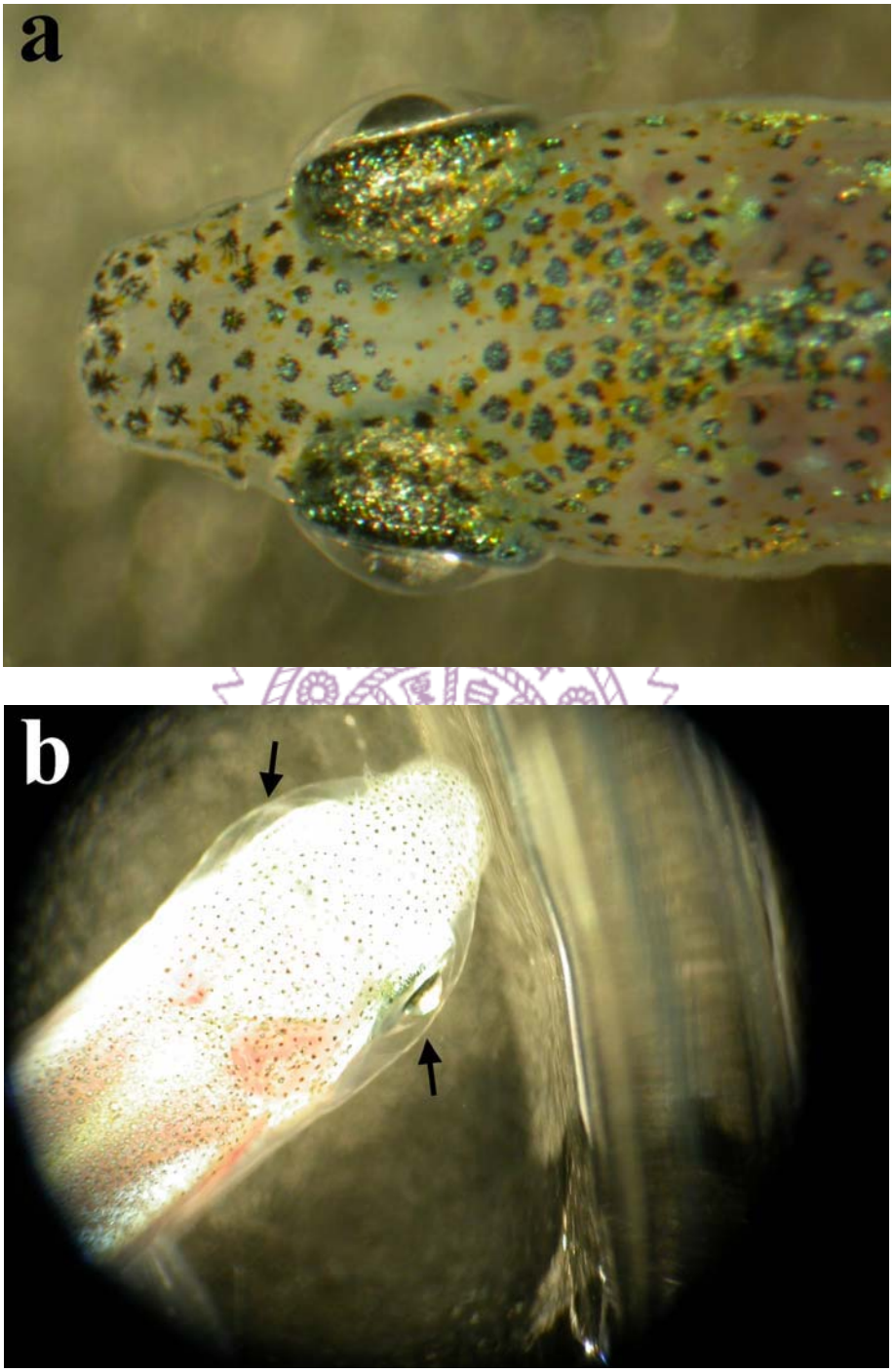

Fig 13. The head region of larval (a) and juvenile milkfish (b) photographed under a dissection microscope. The adipose eyelid is absent in the larval stage but present in the juvenile as indicated by the arrow signs.

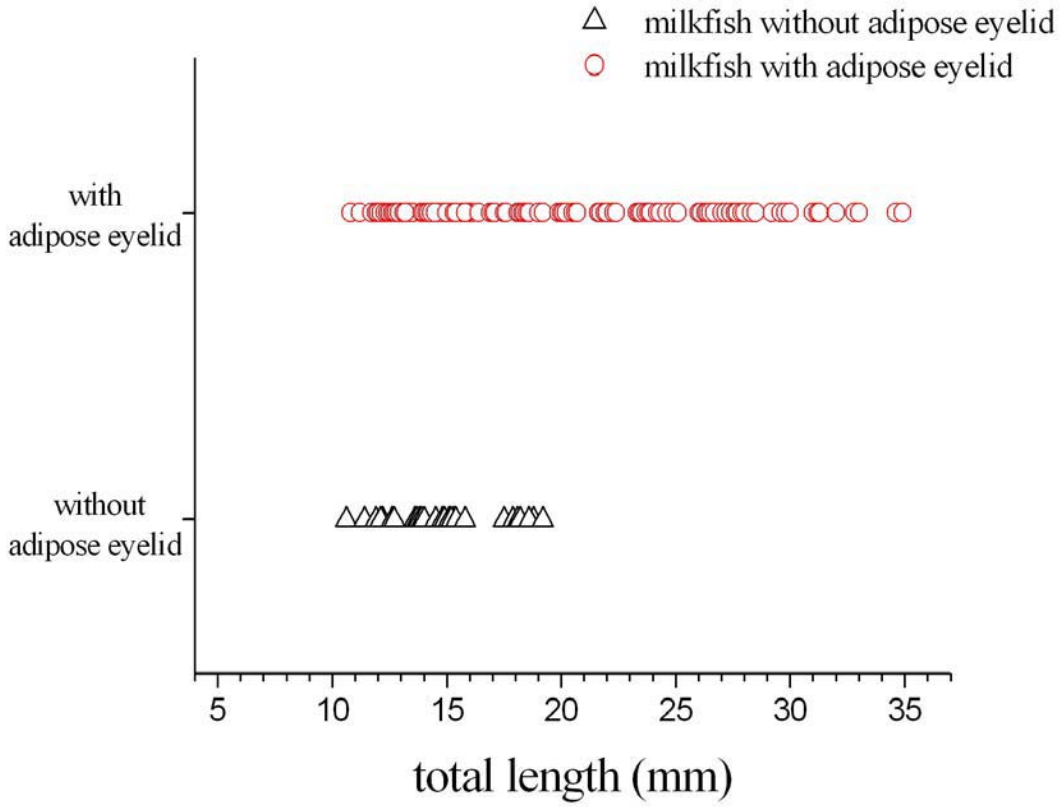

Fig 14. The relationship between total length and the ontogenetic development of the adipose eyelids.

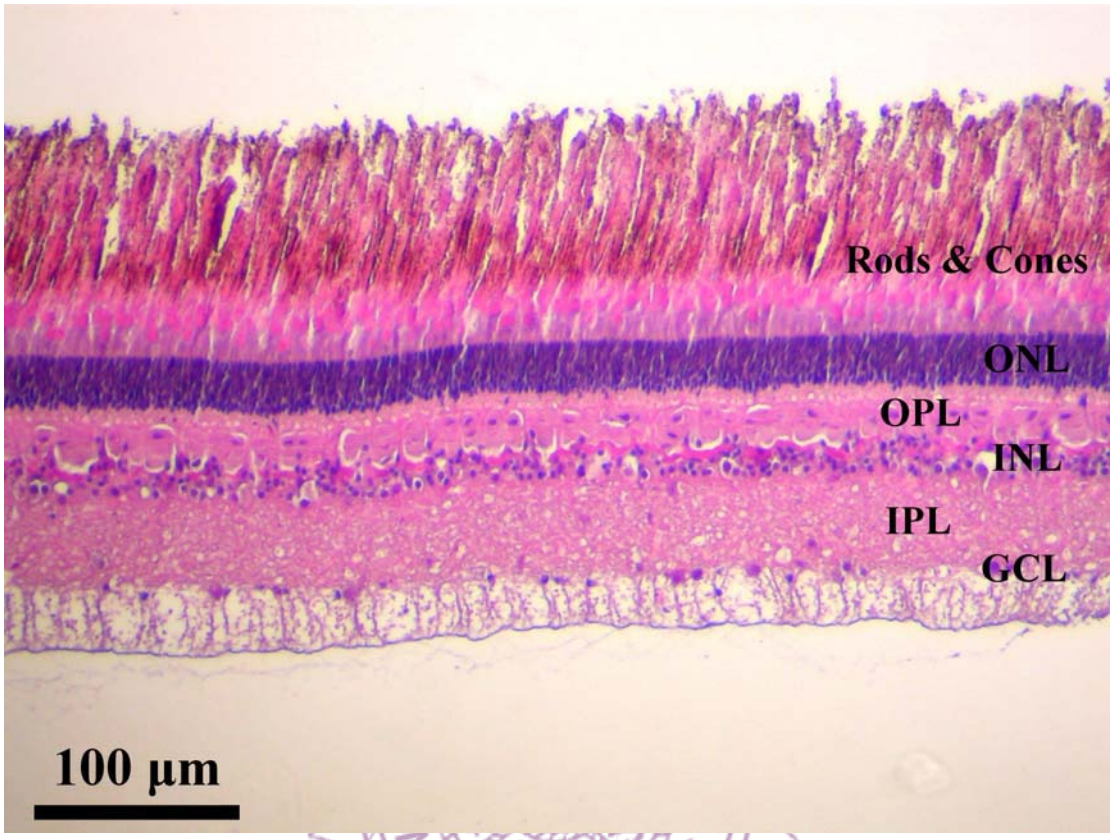

Fig 15. Different layers of retina of the milkfish as revealed by the paraffin section (H&E staining). The Rods & Cones layer contains the outer segments of the photoreceptor cells; the ONL layer contains the cell bodies of the photoreceptor cells; the OPL contains the axons of the photoreceptor cells which synapse with the dendrites of the bipolar cells and horizontal cells; the INL contains the nuclei of bipolar, horizontal, amacrine, and neuroglial Müller's cells; the IPL layer contains the axons of the bipolar cells which synapse with the dendrites of the ganglion and amacrine cells; the GCL layer contains the cell bodies of the neuroglial and ganglion cells.

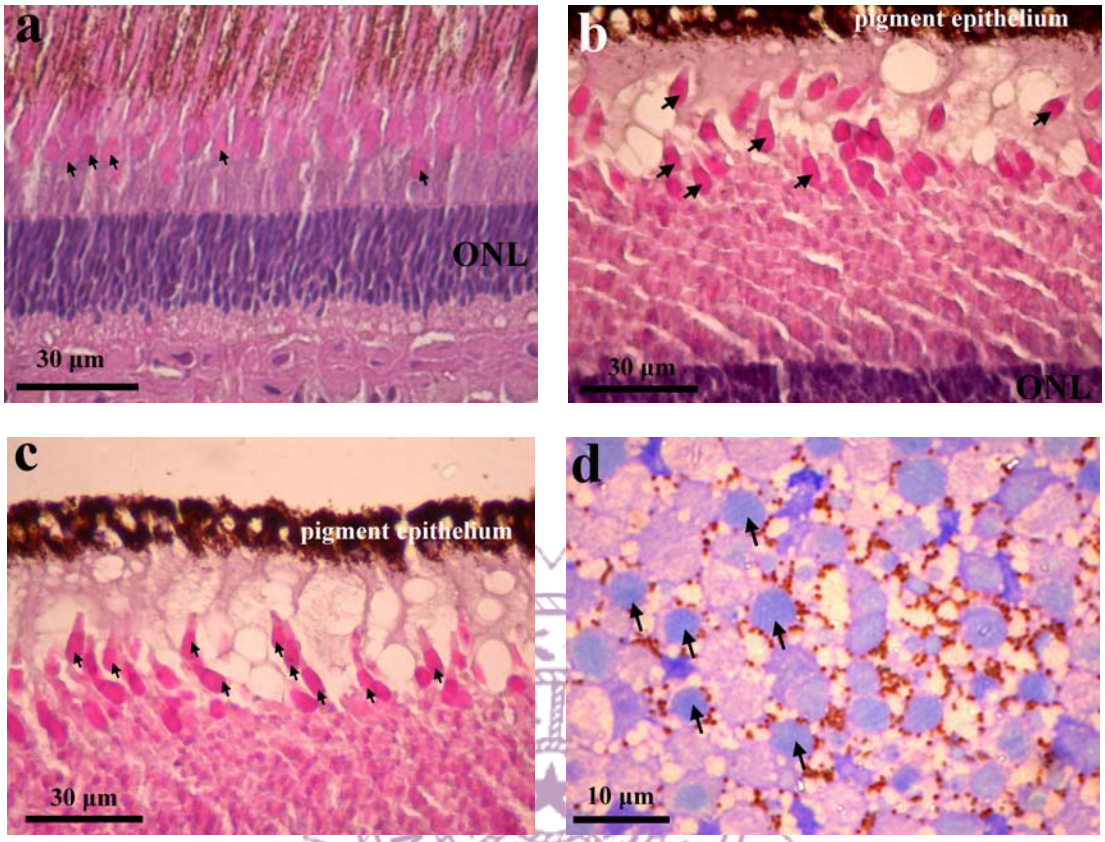

Fig 16. The histological sections of the retina reveal the single cone cells (arrows). (a) The transverse paraffin section of light-adapted retina with H&E staining, (b) The transverse paraffin section of dark-adapted retina with H&E staining, (c) the transverse resin section with H&E staining, (d) the tangential resin section with Toluidine Blue O staining.

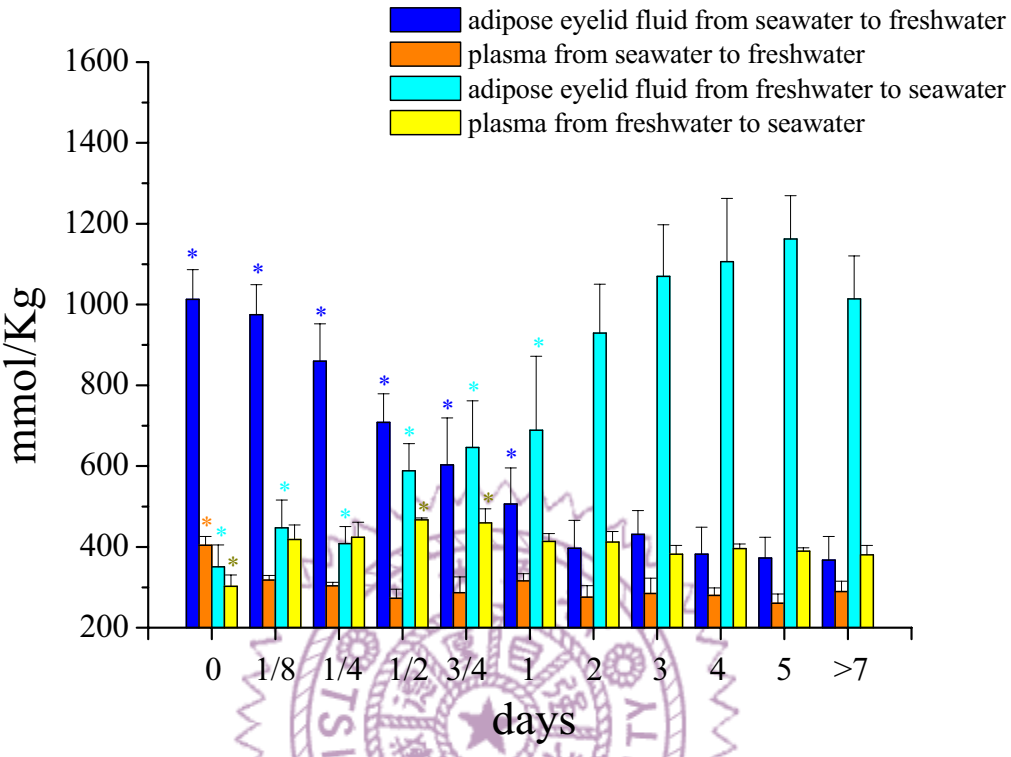

Fig 17. Time-course changes of the plasma and the chamber fluid osmolarities of the milkfish transferred from seawater to freshwater and vice versa. The asterisks indicate the data that were statistically significant different ($P<0.05$) from those of the final data. Values are mean ± S.E.M. (N=6).

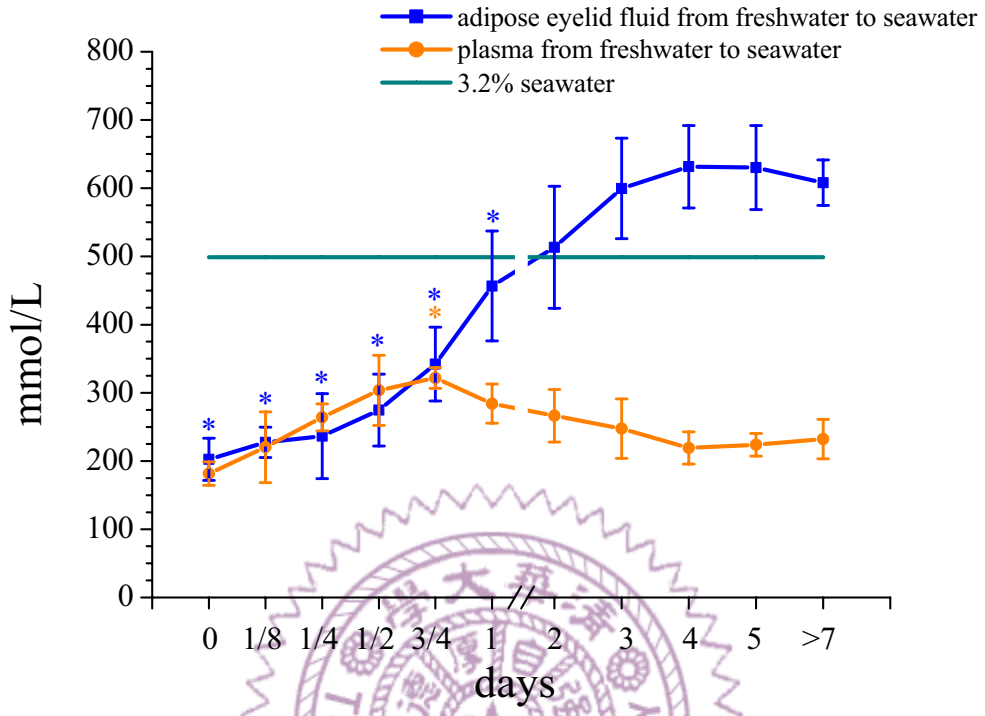

Fig 18. Time-course changes of [Cl^-] in the plasma and the chamber fluid of the milkfish transferred from freshwater to seawater. The asterisks indicate the data that were statistically significant different ($P<0.05$) from those of the final data. Values are mean ± S.E.M. (N=4).

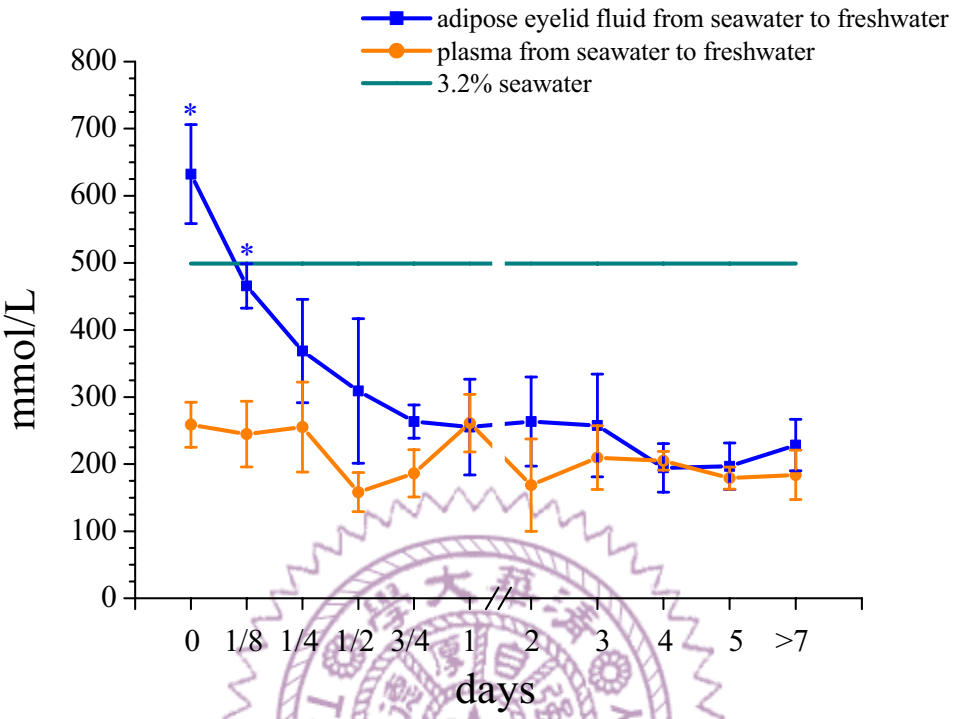

Fig 19. Time-course changes of [Cl^-] in the plasma and the chamber fluid of the milkfish transferred from seawater to freshwater. The asterisks indicate the data that were statistically significant different ($P<0.05$) from those of the final data. Values are mean ± S.E.M. (N=4).

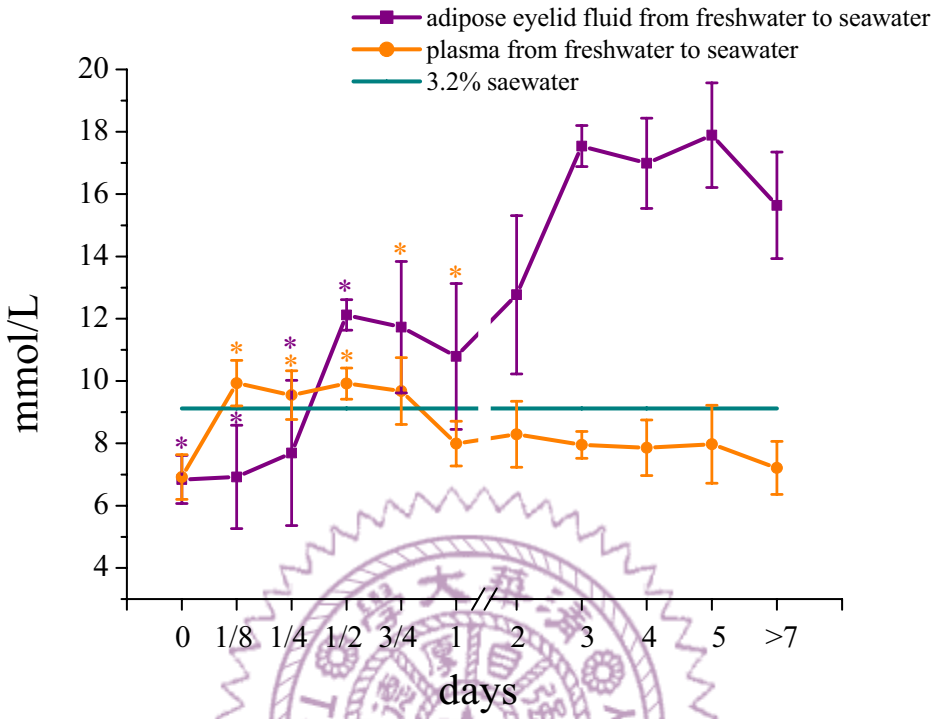

Fig 20. Time-course changes of [K^+] in the plasma and the chamber fluid of the milkfish transferred from freshwater to seawater. The asterisks indicate the data that were statistically significant different ($P<0.05$) from those of the final data. Values are mean ± S.E.M. (N=4).

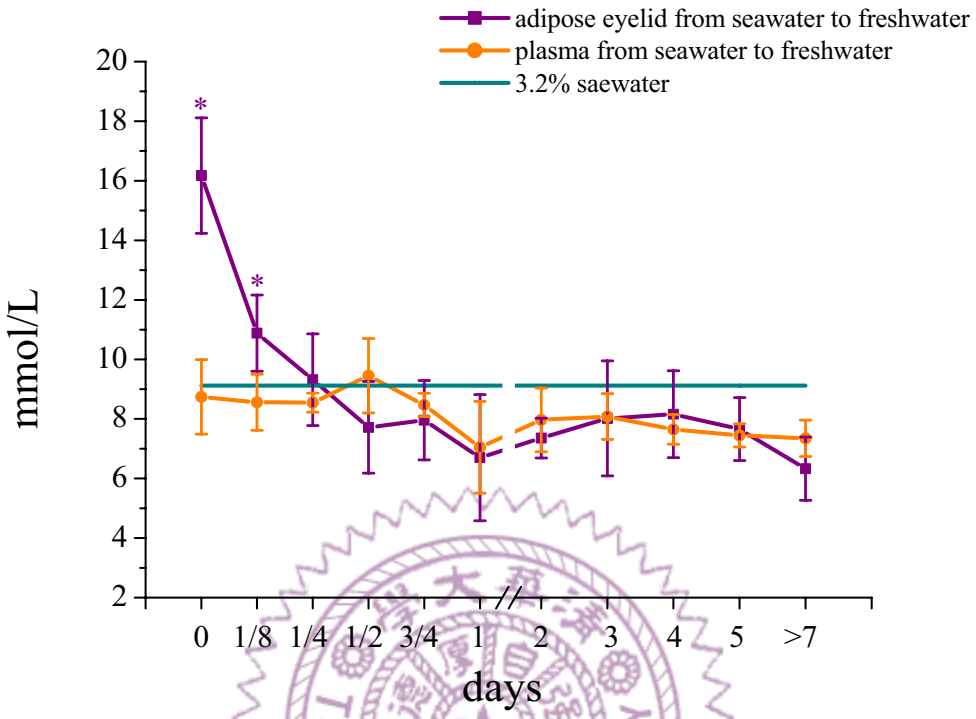

Fig 21. Time-course changes of [K^+] in the plasma and the chamber fluid of the milkfish transferred from seawater to freshwater. The asterisks indicate the data that were statistically significant different ($P<0.05$) from those of the final data. Values are mean ± S.E.M. (N=4).

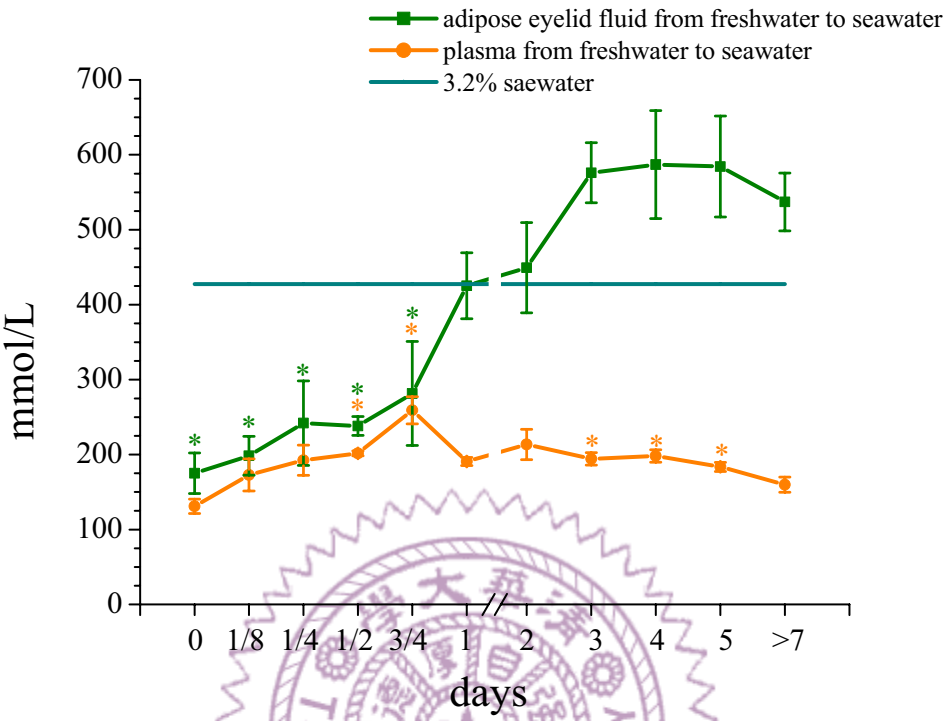

Fig 22. Time-course changes of [Na^+] in the plasma and the chamber fluid of the milkfish transferred from freshwater to seawater. The asterisks indicate the data that were statistically significant different ($P<0.05$) from those of the final data. Values are mean ± S.E.M. (N=4).

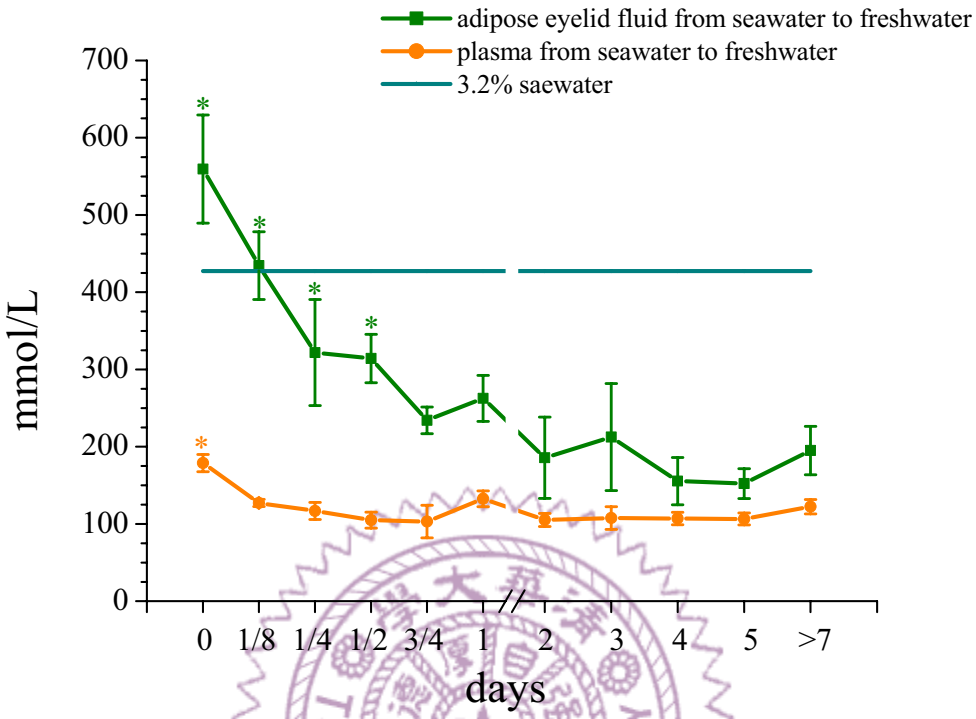

Fig 23. Time-course changes of [Na^+] in the plasma and the chamber fluid of the milkfish transferred from seawater to freshwater. The asterisks indicate the data that were statistically significant different ($P<0.05$) from those of the final data. Values are mean ± S.E.M. (N=4).

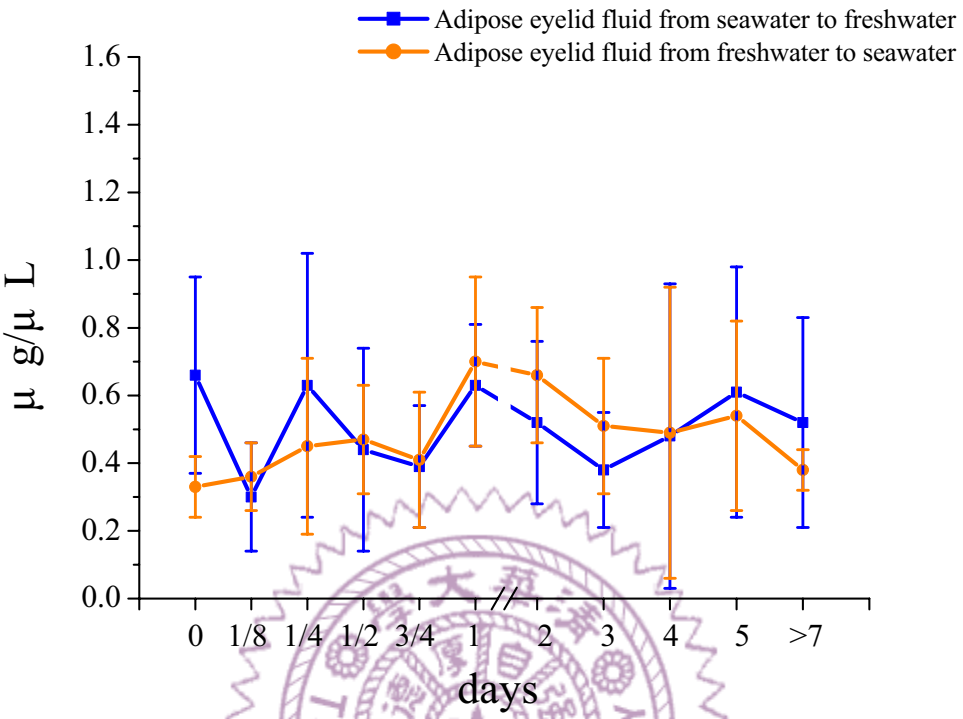

Fig 24. Time-course changes of the protein concentrations of the chamber fluid of the milkfish transferred from freshwater to seawater and vice versa. The asterisks indicate the data that were statistically significant different ($P<0.05$) from those of the final data. Values are mean ± S.E.M. (N=4).

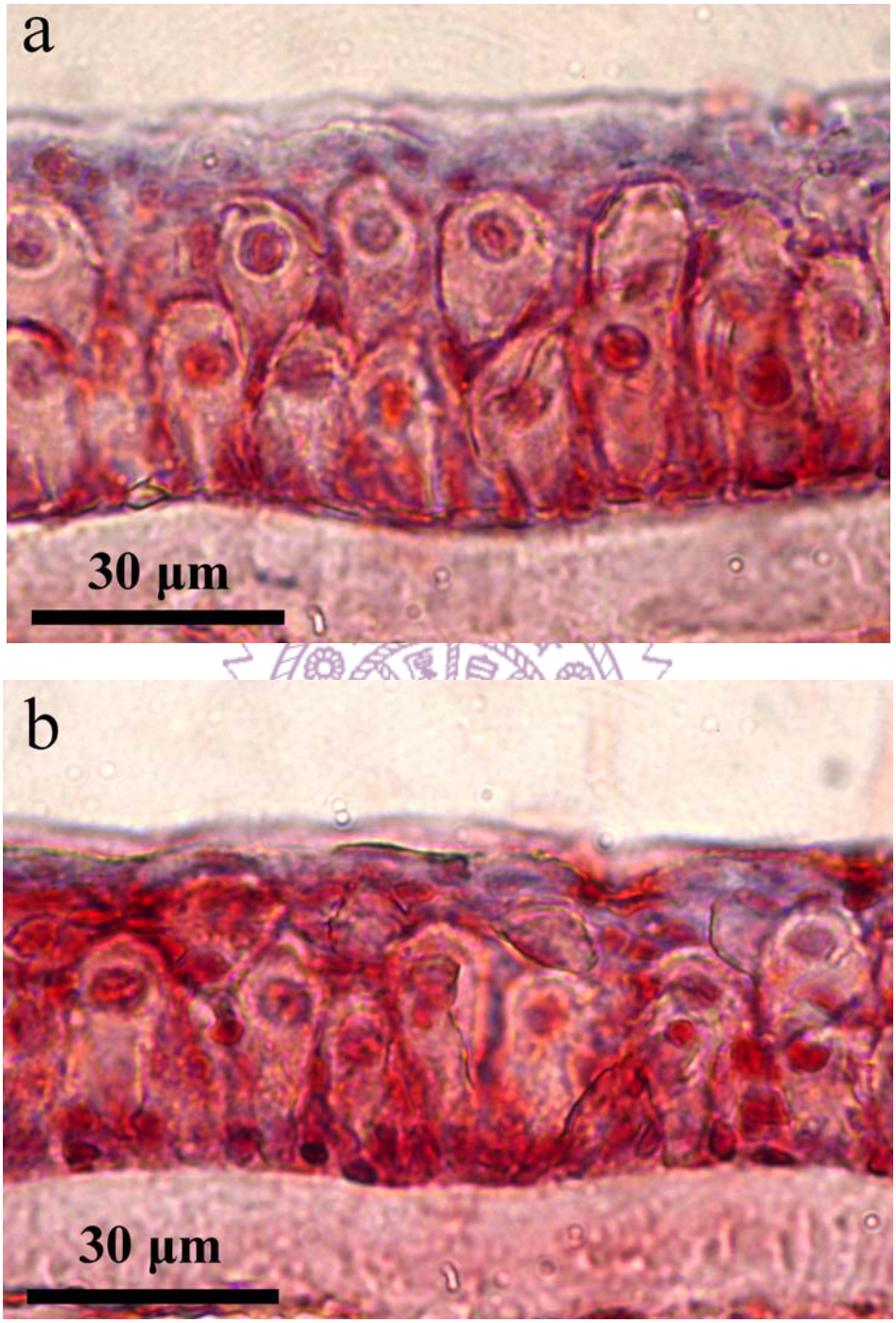

Fig 25. α5 antibody immunostaining in the adipose eyelid of (a) the long-term freshwater adaptation, and (b) long-term seawater adaptation milkfish.

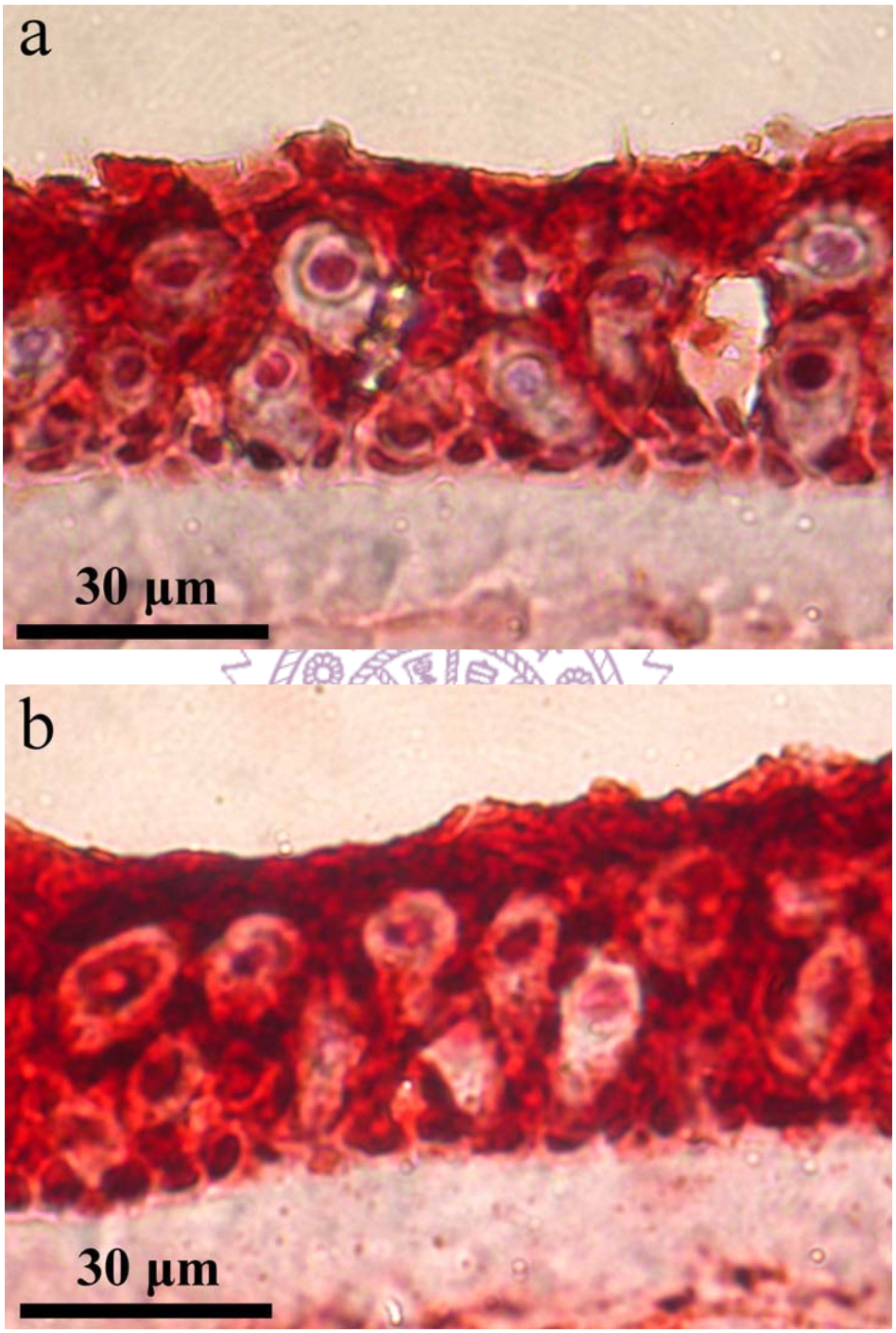

Fig 26. T4 antibody immunostaining in the adipose eyelid of (a) the long-term freshwater adaptation, and (b) long-term seawater adaptation milkfish.

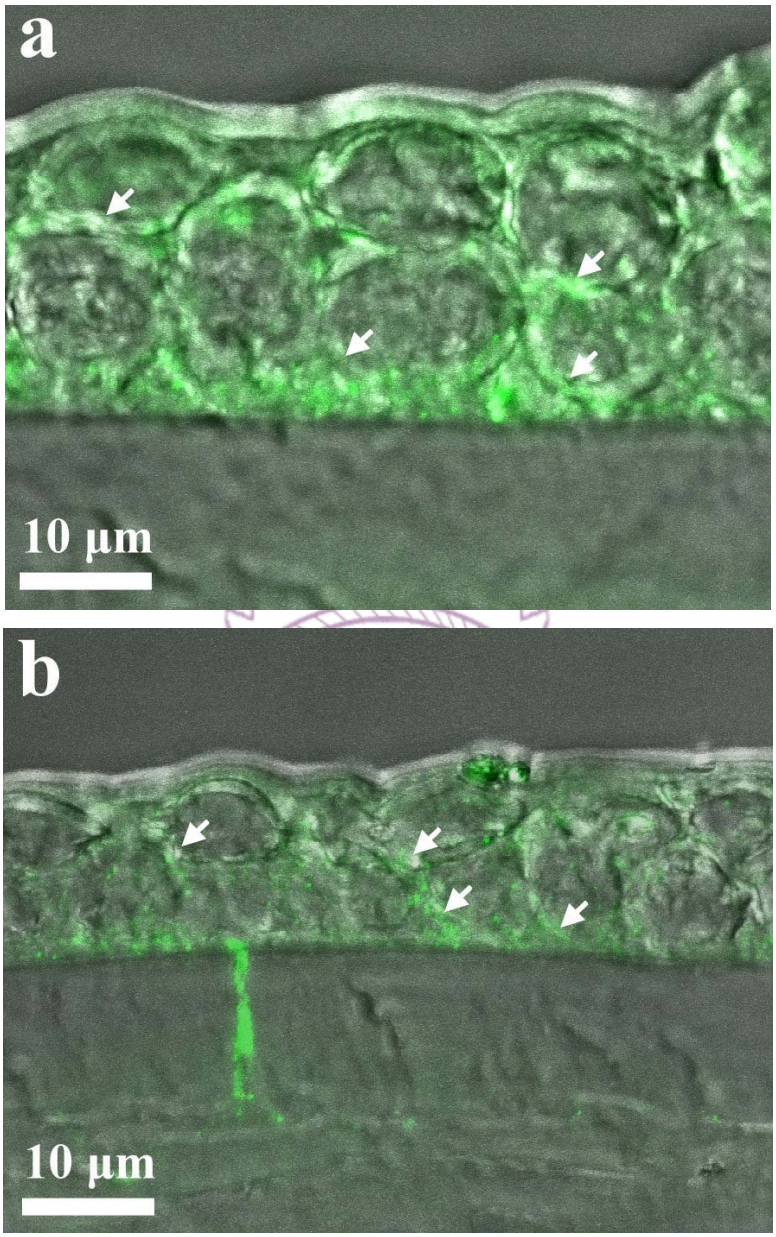

Fig 27. The confocal microphotographs of α5 antibody immunostaining in the adipose eyelid of (a) the long-term freshwater adaptation, and (b) long-term seawater adaptation milkfish. The green parts (as indicated by the arrows) indicate the NKA is expressed in the baselateral membrane of the epithelial cellof the outer multiple epithelium tissue.

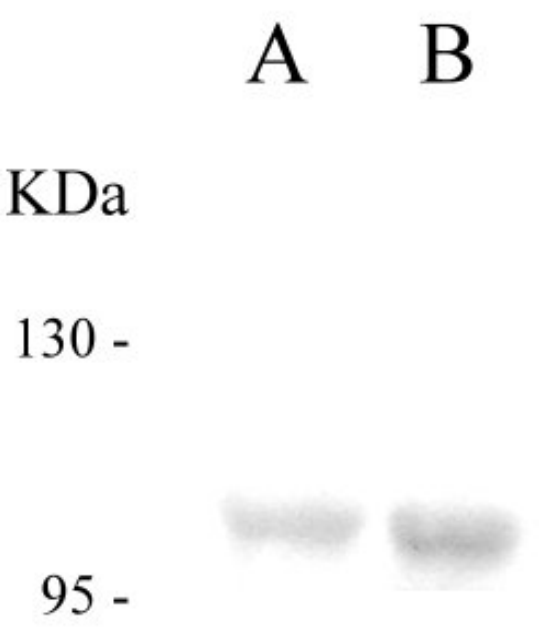

Fig 28. Western blotting of the Na^+/K^+ ATPase α subunit of the milkfish adipose eyelids from (A) long-tern freshwater and (B) seawater adaptation samples.

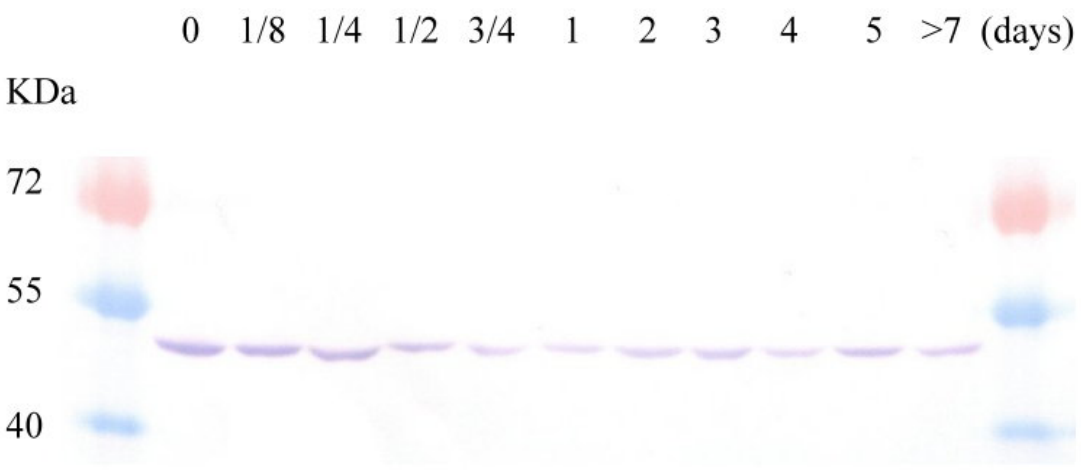

Fig 29. Time course changes of the $Na^+/K^+/Cl^-$(2) cotransporter of the milkfish adipose eyelid when transferred from freshwater to seawater (as revealed by Western blotting).

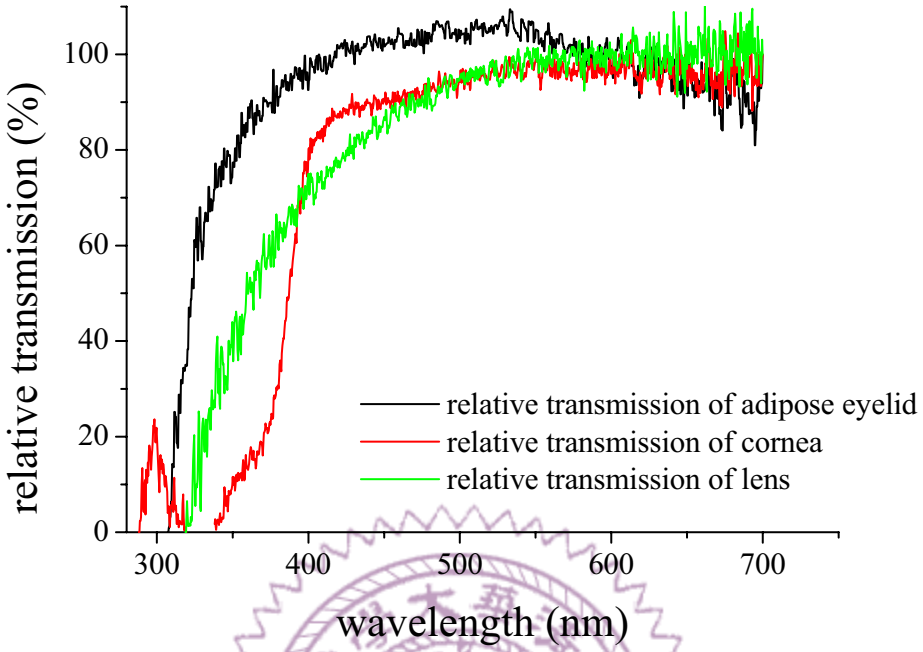

Fig 30. Relative transmission spectra of adipose eyelid (dark line), cornea (red line), and lens (green line) of the juvenile milkfish.

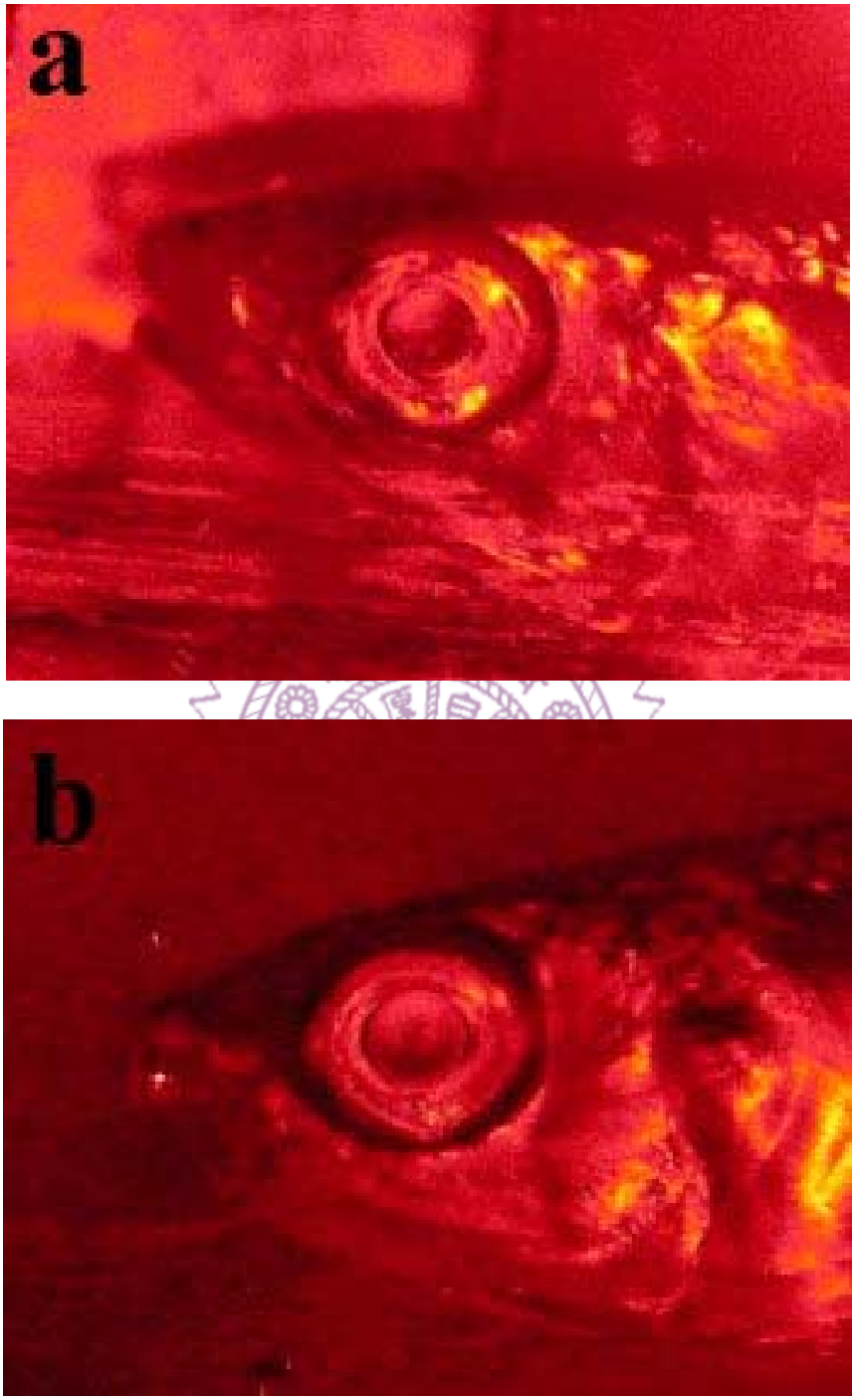

Fig 31. The illuminated area in the milkfish eye. (a) with adipose eyelid, (b) without adipose eyelid.

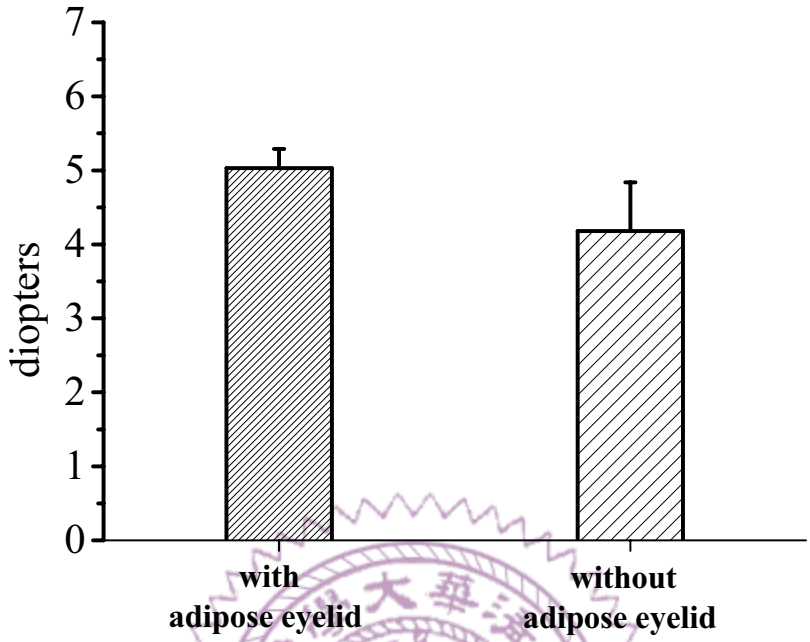

Fig. 32. The diopter values (as measured by a photoretinoscope) of the refractive state of milkfish eye with and without adipose eyelid, values are mean ± S.E.M. (N=4).

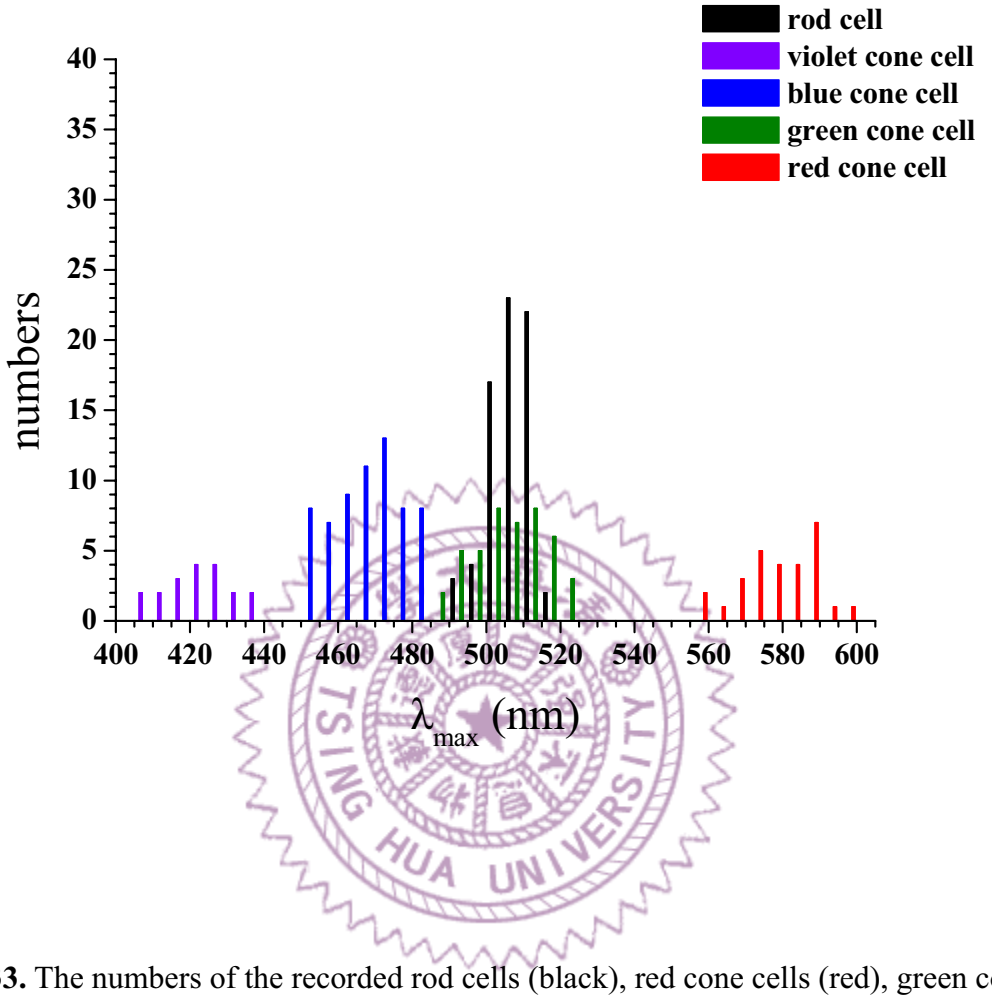

Fig 33. The numbers of the recorded rod cells (black), red cone cells (red), green cone cells (green), blue cone cells (blue), and violet cone cells (violet) and their maximum adsorption wavelength (λ_{max}) values of the larval milkfish retina.

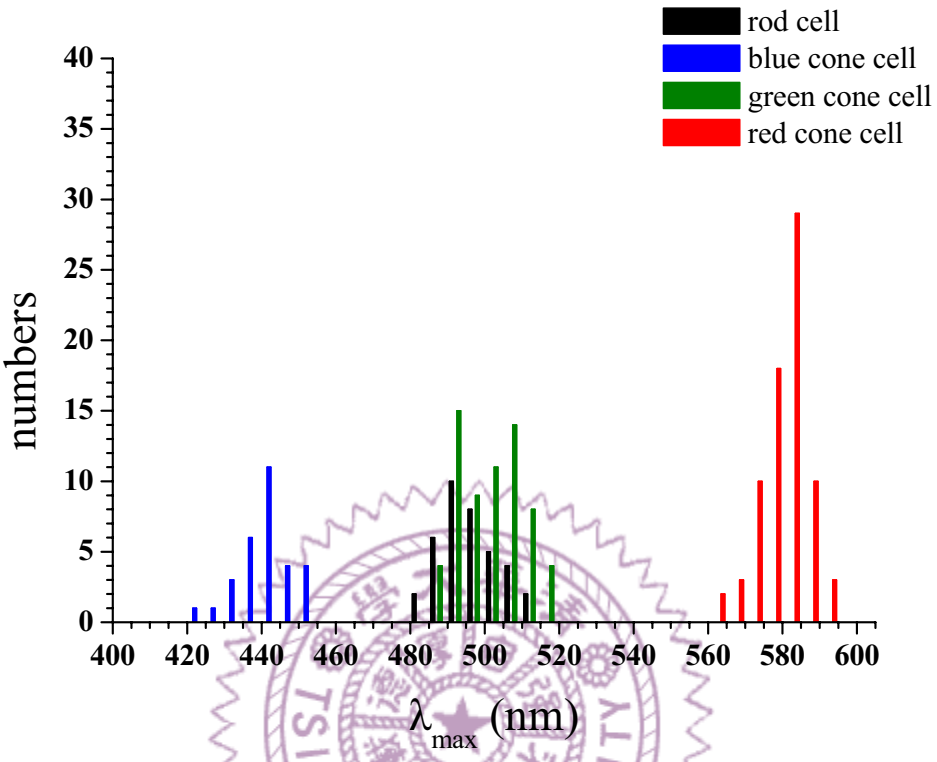

Fig 34. The numbers of the recorded rod cells (black), red cone cells (red), green cone cells (green), and blue cone cells (blue) and their maximum adsorption wavelength (λ_{max}) values of the juvenile milkfish retina.